

DEVELOPMENT OF AN INTEGRATED TECHNOLOGY PACKAGE FOR PADDY STRAW MANAGEMENT

GARIMA SINGH



**CENTRE FOR RURAL DEVELOPMENT AND TECHNOLOGY
INDIAN INSTITUTE OF TECHNOLOGY DELHI
DECEMBER 2022**

© Indian Institute of Technology Delhi (IITD), New Delhi, 2022

DEVELOPMENT OF AN INTEGRATED TECHNOLOGY PACKAGE FOR PADDY STRAW MANAGEMENT

by

GARIMA SINGH

CENTRE FOR RURAL DEVELOPMENT AND TECHNOLOGY

Submitted

**In fulfilment of the requirements of the degree of Doctor of Philosophy
to the**



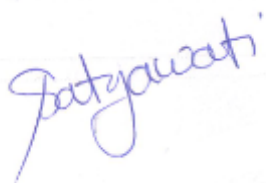
**INDIAN INSTITUTE OF TECHNOLOGY DELHI
DECEMBER 2022**



Dedicated to my
PARENTS

CERTIFICATE

This is to certify that the thesis entitled “**Development of an Integrated Technology Package for Paddy Straw Management**” being submitted by **Ms. Garima Singh** to the **Indian Institute of Technology Delhi** for the award of “**Doctor of Philosophy**” is a record of bonafide research carried by her. She has worked under our supervision and guidance and has fulfilled the requirements for the submission of the thesis. To the best of our knowledge, the results presented in this thesis have not been submitted in part or full to any other institute or university for the award of any degree or diploma.



Dr. Satyawati Sharma

(Professor)

Centre for Rural Development
and Technology

Indian Institute of Technology

Hauz Khas New Delhi-110016

India



Dr. Hariprasad P.

(Associate Professor)

Centre for Rural Development
and Technology

Indian Institute of Technology

Hauz Khas New Delhi-110016

India

ACKNOWLEDGEMENTS

*I bow my head with reverence to Almighty for showering the choicest blessings upon me to bring this PhD work to a holistic end. There have been times in my life when I have been unable to find solutions to my concerns, and the Bhagavat Geeta's teachings of **Lord Krishna** has been my only source of light. The course of the thesis is also the journey of my life, and I express my gratitude to all the people I came across who influenced my life and work.*

*It gives me immense pleasure to express my respect and indebtedness to my supervisor **Prof. Satyawati Sharma** for her motherly affection, co-operation, dedication, and faith in me. Her immense knowledge, positive criticism and encouragement, helped me successfully complete this doctoral thesis. She continually inspired and motivated me to do the best in all the aspects of life and be a better person. I am blessed to have a guide who stood by me in all the phases of my PhD at the professional and personal front. She has been and always be my light, philosopher, and guide. I take this esteemed opportunity in expressing my sincere bouquet of gratitude to my co-supervisor **Prof. Hariprasad P.** for his valuable guidance. His meticulous scrutiny, scholarly advice and scientific approach assisted me to accomplish this work. I sincerely thank him for always helping me find a way out in every critical phase, of my PhD.*

*I would like to extend my gratitude to the honourable members of my research committee **Prof. K.K. Pant** (Chairperson, Department of Chemical Engineering), **Prof. B.J. Alappat** (External expert, Department of Civil Engineering) and **Prof. Vivek Kumar** (Internal expert, CRDT), for their valuable feedback, insightful advice, encouragement, appreciation, and availability. I express my sincere vote of thanks to **Dr. Atul Vyas** and **Dr. Shantanu Roy** for the help, consideration, and availability as and when I approached them.*

*I extend my token of gratitude to office staff **Mrs. Joshi**, **Mrs. Pratibha Rana**, **Mr. Rajendra**, **Mr. Nishant**, **Mr. Chopra** and **CRF staff** for their assistance in every possible way. I am thankful to **Mr. Ramkumar** for his kind help and co-operation throughout my experimental study.*

*I wish to express my cordial thanks to my seniors who always were on my side and uplifted me in every possible way **Dr. Ashwani Kumar**, **Dr. Kanika Chowdhary**, **Dr. Monika Jangir**, **Dr. Shalinee**, and **Dr. Pratibha Yadav**. I sincerely acknowledge **Dr. Himanshi Rathore**, **Dr. Abhishek Sharma**, **Dr. Anurup Adak** and **Dr. Monica Verma** for their help, and valuable suggestions. I would like to take this moment to express my gratitude to my well-wishers,*

colleagues, friends, and everyone I ever met who's been there for me, even if only for a moment, in this roller coaster journey.

Getting through my thesis required more than academic support, and I have many people to thank for listening to and, at times, having to tolerate my mood swings. I am beholden to **Dr. Ranju Sharma, Abhay Tiwari, Mandira Kapri, Dr. Sonal, Mohd. Aamir Khan, Akansha Gupta and Himanshu Arora**. I take this opportunity to pen down and heartfully thank them for being there through all my thick and thins. At times, when I was clueless at any forefront of my life, their assistance was my driving force. I proudly mention that God blessed me with such beautiful souls who are no less than a family to me. I extend my gratitude to **Umesh Rawat, Lahur Mani Verma and Gourav Chowdhir** for their help and motivation. This note might just be a small token of thanks but the support they extended is beyond words.

My heartfelt thanks to my incredibly supportive husband **Himanshu Singh**, who joined me halfway in my doctoral journey. I am grateful to him for all his love, co-operation, and sacrifices. He always motivated me to never give up and keep pursuing my dreams no matter what. All my accomplishments were extremely happy and proud moments for him. I thank him for standing by me in all the situations and utmost for his believe in me. The journey would have been insurmountable without his emotional and moral support.

Finally, I express my deepest gratitude to the wind beneath my wings- my parents and brother. The strongest pillars of my life, **my parents (Shri. Devendra Pratap Singh and Smt. Pushpa Singh)** believed and encouraged me to pursue my dreams. I would never have been able to achieve such heights without their unconditional love, blessings, guidance, and patience. They never let me lose hope and confidence in the most challenging times. No word of thanks will be enough to express the token of thanks to my brother **Mayank**. He was the happiest person on the day I made to PhD at IIT Delhi. He has always been a source of inspiration and my rescuer. I owe this life to my family for all their sacrifices and making me the person I am today. Lastly, to my late grandfather, I wish you could have been here with me today, I hope I made you proud!!

Garima Singh

ABSTRACT

Addressing the concern of stubble burning, the study conducted under this thesis envisages on recycling and reuse of Paddy Straw (PS) to assign a commercial utility to this under-utilized biomass. In this context, a multipronged strategy towards zero waste management of PS by developing value-added products (mushrooms, bioformulations (biopesticides/biofertilizers), nanosilica, and enzymes) was attempted.

Valorization of PS using various de-oiled cakes (DEOCs), depicted that supplementation of 5% soybean cake (SC) gave maximum yield of 1014 g kg⁻¹ *P. ostreatus* fruiting bodies, furnishing an increase of 18.14 % over PS control. Principal component analysis (PCA) performed by analysing the correlation amongst nutritional parameters depicted a total variation of 78.2%. Energy Dispersive X-Ray (EDX) analysis indicated significant increase of minerals in the fruiting bodies and high content of silica (19-20%) in the spent. The cultivation of *T. asperellum* on spent divulged the fact that the fungal growth was comparatively high in spent (14.73*10¹¹) over raw PS (4.2*10³). *T. asperellum* grown on spent showed 66.26% inhibition of *Fusarium oxysporum* compared to the non-supplemented PS spent (54.26%).

In the next part, the Spent Mushroom Substrate (SMS) of *P. ostreatus* was utilized for the development of microbial bioformulations, for plant nutrient and disease management in wilt (*F. oxysporum*) susceptible tomato plant F1 Hybrid King 180. SMS (PS+5% SC) supported the growth of *T. asperellum* (TA) to an extent of 12.37x10¹³ conidia/g substrate. GC-MS analysis of SMS detected several bioactive metabolites known for plant health management. Bioformulations were developed employing Press Mud (PM) and Talcum Powder (TP) as carrier materials. Among the different bioformulations tested in pots study; SMS (PS+5% SC) SiTAPM, collectively named as TF-I, provided improved levels of morpho-biochemical and nutritional parameters, A significant (p<0.05) reduction in the Disease Severity Index (84.34% to 21.23%), was also observed over the pathogen affected plant. The fruits and leaves garnered under TF-I displayed Total Polyphenol Content (TPC) of 74.5 and 126.9 mg/g gallic acid, respectively, with 83.73% DPPH and 72.25% FRAP activity, indicating the elicitation of antioxidant properties. EDX analyses showed 21.53% Silica (Si) in SMS, and plant mapping investigation indicated a substantial accumulation of Si, which is well conceded to promote growth, disease resistance, and antioxidant parameters. The developed bioformulation was delivered to farmers in villages of Uttar Pradesh and a survey study was conducted, which delivered positive outcomes and keen interest towards the implementation of the technology.

An *in-silico* approach was also employed to assess the prospective role of bioactives of *Trichoderma* spp. in combating the *Fusarium* wilt causing enzymes Polygalacturonase (PG2) and tomatinase. The findings of the study revealed that Trichodermamide B produced by *T. harzianum* and Viridin, Virone, and Trichosetin produced by *T. virens* emerged as the potential inhibitors of the phytopathogen's enzymes. MD simulations and MMPBSA confirmed the structural rigidity and stability of the docked complex.

The silica rich straw was further explored for the synthesis of nanosilica (SiNPs) employing the sol-gel method, via integrating the aqueous extract of *Sapindus mukorossi* as surfactant. EDS and FTIR spectra confirmed the predominant peaks of Si and O. FE-SEM confirmed the spheroid morphology of SiNPs with an average particle size of 20.34 ± 2.64 nm as determined by TEM. DLS studies revealed the stability of SiNPs with zeta potential of -14.37 mV and PDI of 0.198, implying its monodispersed nature. BET surface area of SiNPs was recorded as $746.32 \text{ m}^2/\text{g}$ with a cumulative pore volume of $2.059 \text{ cm}^3/\text{g}$. The employment of SiNPs as a carrier material for clove oil (CO), depicted 62.64% encapsulation of CO in SiNPs under UV analysis. The antifungal efficacy of CO-SiNPs against *F. oxysporum* exhibited minimum inhibitory concentration (MIC) of 125 mg/L. The application of SiNPs in photocatalytic degradation of methylene blue reflected that 66.26 % of the dye was degraded in the first 10 mins, and the degradation reflected a first-order kinetics with a half-life of 6.79 mins.

In another objective of this study, PS was explored for lignocellulolytic enzymes under Solid State Fermentation by *Trichoderma* spp. Response Surface Methodology (RSM) optimization of PS in combination with de-oiled neem cake (NC) depicted that PS:NC in 8:3 ratio, provided maximum xylanase activity of 693.56 U/g on the 5th day, with cellulase and laccase activity of 126 U/g and 28.12 U/g, respectively. OHR-LCMS study of the partially purified enzyme revealed the presence of β -xylanase and α -L-arabinofuranosidase. Enzymatic saccharification of various substrates enhanced the release of reducing sugars demonstrating its applicability in the biofuel domain. LC-MS, ICMPS, and EDX profiling of the residual spent unravelled the manifestation of bioactives, minerals, and silica, playing an essential role as biopesticide and biofertilizer. Life Cycle Assessment (LCA) for the SSF process, depicted adverse impacts due to electricity consumption (92.84%) and use of ammonium sulphate salt (6.17%). Nonetheless, employing renewable energy and reducing salt consumption could help minimize these impacts. The findings of the study asserted that PS can be substantially utilized for the development of value-added products. The study also promises new ventures for development of PS based small scale industries, as a source of revenue generation.

शोध का सार

पराली जलाने की समस्या को सम्बन्धित इस शोध के तहत किये गये अध्ययन में धान के पुआल (पीएस) के पुनर्चक्रण और पुनःउपयोग की परिकल्पना की गई है ताकि इस कम उपयोग वाले बायोमास को व्यावसायिक उपयोगिता प्रदान की जा सकें। इस संदर्भ में मूल्यवर्धित उत्पादों जैसे मशरूम, बायोफार्मूलेशन, जैव कीटनाशक / जैव उर्वरक, नैनोसिलिका और एंजाइम विकसित करके धान के पुआल के शून्य अपशिष्ट प्रबंधन की दिशा में एक बहुआयामी रणनीति का प्रयास किया गया है।

विभिन्न डी-आयल्ड केक का उपयोग करते हुए धान के पुआल का वैलोराइजेशन दर्शाता है कि 5% सोयाबीन केक (यससी) के पूरक ने 1014 ग्राम किग्रा⁻¹, पी. ओस्ट्रीट्स फ्रूटिंग बाडी की अधिकतम उपज दी और धान के पुआल नियंत्रण पर 15.14% की वृद्धि दर्ज की। प्रमुख घटक और पोषण संबंधी मापदंडों के बीच सहसंबन्ध का विश्लेषण 78.2% की कुल भिन्नता दर्शाता है। एनर्जी डिस्पर्सिव एक्स-रे (ईडीएक्स) विश्लेषण ने फ्रूटिंग बाडीज में खनिजों की महत्वपूर्ण वृद्धि और खर्च में सिलिका की उच्च सामग्री (19-20%) का संकेत दिया। स्पेंट पर टी. एस्पेरेलम की खेती ने इस तथ्य को उजागर किया कि अपरिष्कृत पीएस (14.73×10^{11}) की तुलना में स्पेंट पीएस (4.2×10^3) में फफूंद वृद्धि तुलनात्मक रूप से अधिक थी। खर्च पर उगाए गये टी0एस्पेरेलम ने गैर-पूरक पीएस खर्च (54.26%) की तुलना में फुसैरियम आक्सीस्पोरम का 66.26% अवरोध दिखाया।

शोध के अगले भाग में, पी. ओस्ट्रीट्स के स्पेंट मशरूम सबस्ट्रेट (एसएमएस) का उपयोग माइक्रोबियल बायोफार्मूलेशन के विकास के लिए किया गया है। पौधे के पोषक तत्व और विल्ट (एफ. आक्सीस्पोरम) से रोग प्रबंधन के लिए अतिसंवेदनशील टमाटर का पौधा एफ-1 हाइब्रिड किंग 180 एसएमएस (पीएस+5% एससी) ने 12.37×10^{13} कोनीडिया/ग्राम सबस्ट्रेट की सीमा तक टी एसपेरेलम (टीए) की वृद्धि का समर्थन किया। एसएमएस के जीसी-एमएस विश्लेषण ने पौधों के स्वास्थ्य प्रबंधन वाले कई बायोएक्टिव मेटाबोलाइट्स का पता लगाया। वाहक सामग्री के रूप में प्रेस मड और टैल्कम पाउडर का उपयोग करके बायोफार्मूलेशन विकसित किए गए थे। बर्तनों में परीक्षण किए गए विभिन्न जैव-सूत्रों के बीच अध्ययन, SMS (PS+5% SC) SiTAPM, एसएमएस (पीएस +5% यससी) SiTAPM जिसे सामूहिक रूप से टीफ-1 नाम दिया गया है, मार्फो-बायोकेमिकल और पोषण संबंधी मापदंडों का बेहतर स्तर प्रदान करता है। रोगजनक प्रभावित पौधे पर रोग गंभीरता सूचकांक (84.34% to 21.23%) में एक महत्वपूर्ण ($p < 0.05$) कमी देखा गया। टीफ-1 के तहत प्राप्त फलों और पत्तियों ने 83.73% (डीपीपीएच) और 72.25% (एफ आर ए पी) गतिविधि के साथ टोटल पालीफेनोल सामग्री (टीपासी) क्रमशः 74.5 और 126.9 मिली / ग्रा0 गैलिक एसिड प्रदर्शित की, जो एंटीआक्सिडेंट गुणों की प्राप्ति का संकेत देती है। ईडीएक्स विश्लेषण ने एसएमएस में 21.53% सिलिका (सी) दिखाया, और प्लांट मैपिंग जांच ने सी के पर्याप्त संचय का संकेत दिया, जो विकास, रोग प्रतिरोध और एंटीआक्सिडेंट पैरामीटर को बढ़ावा देने के लिए अच्छी तरह से माना जाता है। उत्तर प्रदेश के गांवों में विकसित बायोफार्मूलेशन किसानों तक पहुंचाया गया और एक

सर्वेक्षण अध्ययन किया गया, जिसके सकारात्मक परिणाम मिले और प्रौद्योगिकी के कार्यान्वयन में गहरी दिलचस्पी दिखाई दी।

फ्यूजेरियम विल्ट के कारण होने वाले एंजाइम पालीगैलेक्टुरोजेज (पीजी2) और टोमैटिनेज का मुकाबला करने में ट्राइकोडर्मा एसपीपी की बायोएक्टिव्स की संभावित भूमिका का आंकलन करने के लिए एक इन-सिलिको दृष्टिकोण भी नियोजित किया गया था। अध्ययन के निष्कर्षों से पता चला है कि टी. हार्जियानम और विरिडिन, विरोन और टी. वीरेन्स द्वारा उत्पादित ट्राइकोडर्माइड बी फाइटोपैथेजेन के एंजाइमों के संभावित अवरोधक के रूप में उभरा है। एमडी सिमुलेशन और एमएमपीबीयस ने डाकड़ किए गए काम्पलेक्स की संरचनात्मक कठोरता और स्थिरता की पुष्टि की।

नैनोसिलिका (SiNPs) के संश्लेषण के लिए सिलिका समृद्ध पुआल का पता लगाया गया था, जो सपिंडस मुकोरोसी के जलीय अर्क को सर्फैक्ट के रूप में एकीकृत करके सोल-जेल विधि को नियोजित करता है। EDS और STIR LisDV³k ने Si और O की प्रमुख चोटियों की पुष्टि की। FE-SEM ने $20-34 \pm 2-64$ एनएम के औसत कण आकार के साथ के SiNPs गोलाकार आकृति विज्ञान की पुष्टि की, जैसा कि TEM द्वारा निर्धारित किया गया है। डीएलएस अध्ययनों ने -14.37 एमवी की जीटा क्षमता और 0.198 के पीडीआई के साथ एसआईएनपी की सिरिता का खुलासा किया, जो इसकी मोनोडिस्पर्सिड प्रकृति को दर्शाता है। SiNPs का बीईटी सतह क्षेत्र 2.059 सेमी²/जी की संचयी ताकना मात्रा के साथ 746.32 एम²/जी के रूप में दर्ज किया गया था लौंग के तेल (CO) के लिए वाहन सामग्री के रूप में SiNPs का रोजगार, नट विश्लेषण के तहत में SiNPs का CO के 62.64% एनकैप्सुलेशन को दर्शाता है। एफ आक्सीस्पोरम के खिलाफ CO- SiNPs की एंटीफंगल प्रभावकारिता ने 125 mg/L की न्यूनतम निरोधात्मक सांद्रता (MIC) प्रदर्शित की। मेथिलीन ब्लू के फोटोकैटलिटिक डिग्रेडेशन में SiNPs के अनुप्रयोग से परिलक्षित होता है कि पहले 10 मिनट में डाई का 66.26% अवकमित हो गया था, और गिरावट 6.79 मिनट के आधे जीवन के साथ पहले कम के कैनेटीक्स को दर्शाता है।

इस अध्ययन के एक अन्य उद्देश्य में, ट्राइकोडर्मा एसपीपी0 द्वारा ठोस अवस्था किण्वन के तहत लिग्लोसेल्युलोलिटिक एंजाइमों के लिए पीएस की खोज की गई। रिस्पांस सरफेस मेथडोलाजी (RSM) आप्टिइजेशन आफ PS इनकाम्बिनेशन विथ डी-आयल्ड नीम केक (NC) दर्शाता है कि PS:NC 8:3 अनुपात में, सेल्यूलेस और लैकेस एक्टिविटी के साथ 5वें दिन 693.56 U/g की अधिकतम गलसंदेंम गतिविधि प्रदान करता है। क्रमशः 126 यू/जी और 28.12 यू/जी आंशिक रूप से शुद्ध किए गए एंजाइम के OHR-LCMS अध्ययन से β -xylanase और α -L-arabinofuranosidase की उपस्थिति का पता चला। विभिन्न सब्सट्रेट्स के एंजाइमैटिक सैक्रिफिकेशन ने जैव ईंधन डोमेन में इसकी प्रयोज्यता को प्रदर्शित करने वाली शर्करा को कम करने की रिहाइ को बढ़ाया। LC-MS, ICMPs, और EDX खर्च किए गए अवशिष्ट की रूपरेखा ने बायोएक्टिव्स, खनिजों और सिलिका की अभिव्यक्ति को उजागर किया, जो जैव कीटनाशक और जैव उर्वरक के रूप में एक आवश्यक भूमिका निभाते हैं। एसएसएफ प्रक्रिया के लिए जीवन चक्र आकलन (एलसीए), बिजली की खपत (92.84%) और अमोनियम सल्फेट नमक (6.17%) के

उपयोग के कारण प्रतिकूल प्रभाव दर्शाता है। बहरहाल, अक्षय ऊर्जा को रोजगार और नमक की खपत को कम करने से उन प्रभावों को कम करने में मदद मिल सकती है।

अध्ययन के निष्कर्षों यह दावा किया है कि मूल्यवर्धित उत्पादों के विकास के लिए पीएस का काफी हद तक उपयोग किया जा सकता है। अध्ययन राजस्व सृजन के स्रोतों के रूप में पीएस आधारित लघु उद्योगों के विकास के लिए नए उद्योगों का वादा भी करता है।

TABLE OF CONTENTS

Certificate	i
Acknowledgements	ii
Abstract	iv
Table of Contents	v
List of Figures	xi
List of Tables	xvii
List of Abbreviations	xix
Chapter 1	1
1.1	3
1.2	5
1.3	8
1.3.1	9
1.4	10
1.4.1	10
1.4.2	11
1.4.3	12
1.4.4	13
1.5	13
1.5.1	14
1.5.2	15
1.6	20
1.7	24
Chapter 2	25
2.1	25
2.2	26
2.3	27
2.4	30
2.5	33
2.6	36
2.7	36
2.7.1	37
2.7.2	39
2.8	40
2.8.1	41
2.8.2	49
2.8.3	51
2.9	52
2.10	56

2.10.1	Nanosilica in crop life cycle	56
2.10.2	Nanosilica as nanopesticides	57
2.10.3	Nanosilica as nanofertilizers	60
2.10.4	Colloidal Nano delivery systems for the controlled release of pesticides and fertilizers	60
2.11	Potential application of Nanosilica in different domains	67
2.11.1	Catalytic role of Nanosilica in extraction, detection, and degradation of pesticides	67
2.11.2	Nanosilica in photocatalytic treatment of dyes	71
2.12	Toxicity of Nanosilica particles	74
2.13	Bioprospecting techniques for valorization of lignocellulosic biomass	74
2.14	Enzymes	83
2.14.1	Cellulolytic enzymes	83
2.14.2	Hemicellulase enzymes	83
2.14.3	Ligninolytic enzymes	85
2.15	Enzymes production	87
2.16	Life Cycle Assessment	94
2.17	Research gap, Objectives and Work Plan	95
Chapter 3	Valorisation of Paddy Straw for nutraceutical mushroom cultivation and bio-pesticide production	98
3.1	Materials and Methods	99
3.1.1	Materials	99
3.1.2	Experimental setup	99
3.1.3	Chemical analysis of mushroom fruiting bodies	101
3.1.4	Extract preparation of mushroom fruiting bodies obtained under different treatments	101
3.1.5	Estimation of Total Phenolic Content	101
3.1.6	Free Radical Scavenging Activity (DPPH) Assay	102
3.1.7	Ferric Reducing Antioxidant Power (FRAP) Assay	102
3.1.8	Elemental analysis of the fruiting body and spent by Energy Dispersive X-ray Spectroscopy (EDX)	102
3.1.9	FTIR analysis and quantitative estimation of degraded complex molecules in different substrates	102
3.1.10	Cultivation of <i>Trichoderma asperellum</i> on SMS	103
3.1.11	Biocontrol assay: Screening of <i>T. asperellum</i> cultured on different substrates for antagonistic activity against <i>F. oxysporum</i>	103
3.1.12	Statistical analysis	103
3.2	Results and Discussion	104
3.2.1	Physio-chemical properties of Paddy straw and different de-oiled cakes	104
3.2.2	Effect of different substrates on yield and biological efficiency of <i>P. ostreatus</i>	104
3.2.3	Effect of different substrates on nutritional composition of <i>P. ostreatus</i>	106

3.2.4	Effect of different substrates on antioxidant properties of methanolic extracts of <i>P. ostreatus</i>	108
3.2.5	EDX analysis of mineral uptake in <i>P. ostreatus</i>	111
3.2.6	EDX analysis of minerals in spent mushroom substrate (SMS)	113
3.2.7	FTIR analysis of spent mushroom substrate	113
3.2.8	Growth study of <i>T. asperellum</i> on different substrate combinations and study of its efficacy towards control of <i>Fusarium oxysporum</i>	115
3.3	Cost calculation of <i>P. ostreatus</i> cultivation on PS	117
3.4	Conclusion	118
Chapter 4	Development of bio-formulations using <i>Trichoderma asperellum</i> enriched silica-rich Spent Mushroom Substrate for plant health and disease management against <i>Fusarium</i> wilt in tomato plants (<i>In planta</i> and <i>In silico</i> studies)	119
4.1	Materials and Methods	120
4.1.1	Procurement of materials	120
4.1.2	Physicochemical characterization of the substrates	121
4.1.3	Solid State Fermentation (SSF) of substrates using <i>T. asperellum</i>	121
4.1.4	Morphological characterization of substrates	121
4.1.5	Gas Chromatography Mass Spectroscopy (GC-MS) of the substrates	121
4.1.6	Development and shelf-life study of PM and TP based bioformulations	122
4.1.7	Effect of different bioformulations on seed germination	122
4.1.8	Mass multiplication of the plant pathogen (<i>Fusarium oxysporum</i>)	123
4.1.9	<i>In planta</i> assay	123
4.1.10	Measurement of Disease Severity Index (DSI)	125
4.1.11	Evaluation of plant biochemical, growth and generative parameters	125
4.1.12	Estimation of nutritional and nutraceutical parameters of the ripened tomato fruits	126
4.1.13	Estimation of antioxidant properties of tomato fruits and leaves	128
4.1.13.1	Estimation of Total Phenolic Content (TPC)	128
4.1.13.2	DPPH Radical Scavenging (DPPH) and Ferric Reducing Antioxidant Power (FRAP) assay	128
4.1.14	Nutrient content analyses of tomato plants	128
4.1.15	Statistical Analysis	128
4.2	Results and Discussion	129
4.2.1	Physicochemical properties of the substrates	129
4.2.2	Morphological characteristics of the biodegraded substrates	129
4.2.3	GC-MS analysis of <i>T. asperellum</i> treated substrates	130
4.2.4	Shelf-life study of developed bioformulations	135
4.2.5	Germination percentage of tomato seeds	136
4.2.6	Disease Severity Index	137
4.2.7	Plant Biochemical parameters	139
4.2.8	Plant growth and generative parameters	140
4.2.9	Nutritional and nutraceutical properties of tomato plant	142

4.2.9.1	Effect of different treatments on Carbohydrates, TSP, and TSS content	142
4.2.9.2	Effect of different treatments on nutraceutical parameters	142
4.2.10	TPC of tomato fruits and leaves	144
4.2.11	Antioxidant activity of tomato fruit extracts obtained under different treatments	145
4.2.12	Silica content in SMS and tomato plants analysed using EDS	149
4.3	Field Study	151
4.4	Conclusion (<i>In planta</i>)	154
4.5	Deciphering the role of <i>Trichoderma</i> sp. bioactives in combating the enzymes causing <i>Fusarium</i> wilt: An <i>in-silico</i> approach	155
4.5.1	Materials and Methods	156
4.5.1.1	Materials	156
4.5.1.2	Homology modelling and structure evaluation	156
4.5.1.3	Ligand and Protein structure preparation	157
4.5.1.4	Molecular Docking: Virtual Screening of Molecules	157
4.5.1.5	Dual culture assay of <i>Trichoderma</i> sp. with <i>F. oxysporum</i>	158
4.5.1.6	Molecular dynamics simulations of docked complexes	159
4.5.1.7	Free binding energy analysis: Molecular Mechanic/Poisson Boltzmann surface area (MM-PBSA)	159
4.5.2	Results and Discussion	161
4.5.2.1	Homology modeling and Structural Validation	161
4.5.2.2	Molecular docking of <i>Fusarium</i> enzymes with bioactive metabolites of <i>Trichoderma</i> sp.	165
4.5.2.3	Interaction study of <i>Trichoderma</i> sp. and <i>F. oxysporum</i> (<i>In vitro</i>)	169
4.5.2.4	Molecular dynamics simulation	170
4.5.2.4.1	Root Mean Square Deviation (RMSD)	170
4.5.2.4.2	Root Mean Square Fluctuation (RMSF)	172
4.5.2.4.3	Radius of gyration (Rg) analysis	174
4.5.2.4.4	Solvent accessible surface area (SASA)	175
4.5.2.4.4	Hydrogen bond formation	176
4.5.2.5	Free Binding Energy Analysis	177
4.5.3	Conclusion (<i>In silico</i>)	178
Chapter 5	Bioinspired fabrication of Nanosilica using Paddy straw and its potential application in different sectors	179
5.1	Materials and Methods	181
5.1.1	Materials	181
5.1.2	Preparation of Paddy Straw Ash	181
5.1.3	Nano silica extraction from rice straw ash	182
5.1.4	Extraction of Nanosilica from paddy straw ash employing <i>S. mukorossi</i> seed aqueous extract	183
5.1.5	Preparation and characterization of <i>Sapindus mukorossi</i> seed pericarp aqueous extract	184

5.1.6	Characterization of Paddy Straw ash and Nanosilica powders	185
5.1.6.1	UV Vis spectra of SiNPs	185
5.1.6.2	X-ray Diffraction (XRD) analysis	185
5.1.6.3	Fourier transform infrared spectroscopy (FTIR) analysis	185
5.1.6.4	Morphological studies	185
5.1.6.5	Surface Area and Porosity	186
5.1.6.6	Contact angle and stability of SiNPs	186
5.1.7	Essential oil loading in Nanosilica	186
5.1.7.1	Essential oil encapsulation efficiency of SiNPs	186
5.1.7.2	<i>In-vitro</i> antifungal assay	187
5.1.8	Application of Nanosilica in photocatalytic degradation of cationic dye	188
5.2	Results and Discussion	188
5.2.1	Characteristics of PS ash	188
5.2.2	Characteristics of <i>Sapindus mukorossi</i> aqueous extract	191
5.2.3	Characteristics of Silica Nanoparticles	192
5.2.3.1	UV-Vis spectrophotometry	192
5.2.3.2	XRD Spectra	193
5.2.3.3	FTIR Spectra	194
5.2.3.4	EDX Spectra	196
5.2.3.5	Morphological properties	197
5.2.3.5.1	FESEM, TEM and AFM	197
5.2.3.6	BET surface area of Nanosilica	200
5.2.3.7	DLS, TGA and Contact angle study for SiNPs	201
5.2.4	Encapsulation of essential clove oil in SiNPs	202
5.2.4.1	Study on controlled release behaviour of CO-SiNPs for combating phytopathogens	204
5.2.5	Decolorization of cationic dye methylene blue using amorphous SiNPs	206
5.2.5.1	Kinetic study of dye degradation	207
5.2.5.2	FTIR studies of methylene blue decolorization	208
5.3	Economic assessment of SiNPs	210
5.4	Conclusion	211
Chapter 6	Harnessing the potential of Paddy straw for production of lignocellulolytic enzymes under Solid State Fermentation	212
6.1	Materials and Methods	214
6.1.1	Procurement of cultures	214
6.1.2	Screening of <i>Trichoderma</i> spp. for lignocellulolytic enzyme production	214
6.1.2.1	Enzymatic assay	215
6.1.2.2	Solid-state fermentation (SSF)	216
6.1.2.3	Monitoring of fungal growth during SSF by glucosamine estimation	216
6.1.3	Optimization of culture conditions for enzymatic production	217
6.1.4	Enzyme extraction and assay	218

6.1.5	Total protein estimation of enzymatic extract	219
6.1.6	Partial Purification of the crude enzymatic extract	220
6.1.7	OHR-LCMS analysis of the proteins obtained from SDS Gel	220
6.1.8	Characterization of partially purified enzyme extract	221
6.1.8.1	Temperature and pH	221
6.1.8.2	Enzyme kinetics	221
6.1.9	Enzymatic saccharification of lignocellulosic substrates	222
6.1.10	Characterisation of residual spent	222
6.1.10.1	Structural and chemical changes in biotreated substrates	222
6.1.10.2	GCMS analysis of residual spent (volatile components)	222
6.1.10.3	LCMS analysis of residual spent (non-volatile components)	222
6.1.11	Statistical analysis	223
6.1.12	LCA: Goal, Scope, and Function unit	223
6.1.12.1	LCA Methodology	225
6.2	Results & Discussion	227
6.2.1	Screening of the strains for production of lignocellulolytic enzymes	227
6.2.2	Chitin content of fungal strains	230
6.2.3	RSM optimized results for lignocellulolytic enzymes production	231
6.2.4	Partial purification of crude enzymatic extract	237
6.2.5	Identification of the proteins by OHR-LCMS	239
6.2.6	Effect of physiochemical parameters on xylanase activity	241
6.2.7	Enzyme saccharification	244
6.2.8	LCA for xylanase enzyme	245
6.2.9	Spent characteristics	249
6.2.9.1	Morphological, chemical, and structural modifications of the spent substrate	249
6.2.9.2	Residual Paddy straw as a source of bioactives by GCMS	252
6.2.9.3	Residual Paddy straw as a source of bioactives by LCMS	258
6.2.9.4	Residual Paddy straw as a source of minerals and silica	266
6.3	Conclusion	267
Chapter 7	Conclusion and Future Prospective	271
	References	273
	Appendices	329
	Biodata	366

LIST OF FIGURES

FIGURE	PARTICULAR (S)	PAGE
Fig. 1.1	Crops cultivated in India	1
Fig. 1.2	Leading countries for rice production	2
Fig. 1.3	Paddy cultivation area and production in India	3
Fig. 1.4	Classification of Paddy plant	4
Fig. 1.5	Calvin cycle of Paddy plant	4
Fig. 1.6	Crop residues generated in India	6
Fig. 1.7	Statistical representation for annual crops produced, residues generated, and burnt from 2003-04 to 2016-17	7
Fig. 1.8	Contribution of various crop residues burnt in India	7
Fig. 1.9	Current Paddy straw management strategies	8
Fig. 1.10	Factors contributing to stubble burning	9
Fig. 1.11	A. Paddy straw burning B. VIRRS image as recorded by NASA	10
Fig. 1.12	Impacts due to stubble burning	12
Fig. 1.13	Paddy straw management techniques	13
Fig.1.14	Timeline depicting critical intervention to mitigate stable burning in India	23
Fig. 2.1	Structural representation of linkage of cellulose, hemicellulose, and lignin	25
Fig. 2.2	Uptake mechanism of Silica in paddy plants	27
Fig. 2.3	World mushroom production	28
Fig. 2.4	World mushroom consumption	28
Fig. 2.5	Status of mushroom cultivation in different states of India and percentage hold of various mushrooms	29
Fig. 2.6.	Percentage hold of various mushrooms in India.	29
Fig. 2.7	Various applications of deoiled cakes in different sectors	32
Fig. 2.8	Various applications of Spent Mushroom Substrate	33
Fig. 2.9	Life cycle of <i>F. oxysporum</i>	38
Fig. 2.10	Types of pesticides used in agriculture domain	40
Fig. 2.11	Mechanism of <i>Trichoderma</i> spp. in combating phytopathogen attack	42
Fig. 2.12	Types of microbial formulations and its associated properties	50
Fig. 2.13	Use of Nanosilica as a carrier agent	64
Fig. 2.14	Use of Nanosilica in pesticide detection, degradation, and removal	68
Fig. 2.15	Schematic representation of photocatalytic mechanism of methylene blue degradation by SiNPs	72
Fig. 2.16	Different applications of lignocellulosic fractions of plant biomass	75
Fig. 2.17	Various pre-treatment methods of lignocellulosic biomass	76
Fig. 3.1	Flowchart indicating the valorization of PS for nutraceutical mushroom cultivation and bio-pesticide production.	99
Fig. 3.2	Biological efficiency of <i>P. ostreatus</i> cultivated on Paddy straw supplemented with different percentages of de-oiled cakes.	106
Fig. 3.3	Principal Component Analysis of nutritional (fats, protein, carbohydrates, fibre, and ash) composition of fruit bodies harvested from different treatments	108

Fig. 3.4	Free Radical Scavenging Activity of different methanolic extracts of <i>P. ostreatus</i> fruiting body harvested from different treatments by DPPH at varying concentrations.	110
Fig. 3.5	Ferric Reducing Antioxidant Power of different methanolic extracts of <i>P. ostreatus</i> fruiting body harvested from different treatments.	110
Fig. 3.6	Comparison of Element weight (%) in <i>P. ostreatus</i> fruit bodies obtained from different substrate combinations using EDX analysis.	112
Fig. 3.7	Comparison of element weight (%) in spent mushroom substrate obtained from different substrate combinations using EDX analysis.	113
Fig. 3.8	FTIR spectra of spent mushroom substrate and untreated Paddy straw	115
Fig. 3.9	Antagonist effect of <i>Trichoderma asperellum</i> cultivated on Spent mushroom substrate against <i>Fusarium oxysporum</i> . a: <i>F. oxysporum</i> (control) mycelia growth; b: <i>F. oxysporum</i> mycelia growth on Paddy straw spent; c: <i>F. oxysporum</i> mycelia growth on Paddy straw + Soybean cake spent	116
Fig. 4.1	Schematic representation for development of Bioformulations using Spent Mushroom Substrate and <i>In Planta</i> assay against <i>Fusarium</i> wilt in tomato	120
Fig. 4.2	Experimental layout for development of bioformulations and <i>In Planta</i> assay	123
Fig. 4.3	Tomato plants under different treatments in flowering and fruiting stage	126
Fig. 4.4	FE-SEM micrographs at a magnification of 2500 and EHT 20 kV (A) . Raw Paddy straw (PS) (B) . SMS of <i>P. ostreatus</i> (C) . SMS (PS+ 5% SC) of <i>P. ostreatus</i> (D) . <i>T. asperellum</i> cultivated on Raw PS (E) . <i>T. asperellum</i> cultivated on SMS (PS) (F) . <i>T. asperellum</i> cultivated on SMS (PS+5%SC)	130
Fig. 4.5	Viability of <i>Trichoderma asperellum</i> (cfu/g) of developed bioformulations.	135
Fig. 4.6	Germination rate (%) of tomato seeds upon treatments with bioformulations (T1-T6) in comparison to control without any seed coating after 15 days.	137
Fig. 4.7	Disease Severity Index representing the percentage of wilting caused by <i>F. oxysporum</i> under the effect of different treatments, calculated based on hedonic scale	138
Fig. 4.8	Effect of different treatments (A) . Chlorophyll a (chl-a) and Chlorophyll b (chl-b) content in tomato leaves (B) . Carotenoid contents of tomato leaves	139
Fig. 4.9	Effect of different treatments on (A) . Plant Biomass (B) . Plant Height (C) . Fruit Biomass (D) . Fruit Numbers. The values represent per plant data, expressed as Mean \pm SD for experiments conducted in triplicates. Different letters denote significant difference at $p < 0.05$ by Tukey's multiple range test. (E) . Schematic representation for roots of tomato plants obtained under different treatments.	141
Fig. 4.10	Effect of different treatments on nutritional and nutraceutical quality of ripe tomato fruits at harvest (A) . Total Carbohydrates (B) . Total Soluble Proteins (TSP) (C) . Lycopene (D) . Total Soluble Sugars (TSS) (E) . Ascorbic acid (AA) (F) . β -carotene.	143

Fig. 4.11	Total Phenolic Contents of tomato fruits and leaves treated with different treatments	145
Fig. 4.12	DPPH Scavenging Activity and FRAP antioxidant for tomato fruit extracts.	146
Fig. 4.13	(A) . EDX analyses of SMS (PS+5%SC) illustrating the micronutrients and macronutrients content. (C) . EDX analysis of tomato leaves (D) . EDX analysis of tomato fruits (E) . FE-SEM micrographs (3000 magnification and EHT of 20 kV) depicting Si in leaves (F) . EDX mapping representing the accumulation of Si in different parts of tomato leaves (G) . FE-SEM micrographs (3000 magnification and EHT of 20 kV) showing traces of Si presence in tomato fruits (H) . EDX mapping depicting traces of Si in different sections of tomato fruits.	150
Fig.4.14	Plate of Technology dissemination in rural sectors of different villages of Uttar Pradesh.	151
Fig.4.5.1	Flow chart of the pipeline applied in present study to identify the bioactive metabolites of <i>Trichoderma</i> spp. as potential inhibitor against <i>Fusarium</i> enzymes	156
Fig.4.5.2	(A) 3D structure and structure evaluation of tomatinase protein rendered using the UCSF Chimera (B) Ramachandran plots of modelled 3D structure of tomatinase (C) 3D structure and structure evaluation of PG2 protein (D) Ramachandran plots of modelled 3D structure of PG2	163
Fig.4.5.3	Schematic representation of molecular docking results (a) Modelled 3D structure of Tomatinase structure predicted using homology modelling-based approach (b) 2D interaction representation between tomatinase and Virone (c) Interaction between tomatinase and Trichosetin (d) Interaction between Tomatinase and Trichodermamide B	166
Fig.4.5.4	Schematic representation of molecular docking results (a) Modeled 3D structure of PG2 structure predicted using homology modeling-based approach; (b) 2D interaction representation between PG2 and Trichodermamide B (c) Interaction between PG2 and Viridin (d) Interaction between PG2 and Virone (e) Interaction between PG2 and Trichosetin	167
Fig.4.5.5	Control plates (a) <i>Fusarium oxysporum</i> (b) <i>Trichoderma virens</i> (c) <i>Trichoderma harzianum</i> . Dual culture assay of <i>F. oxysporum</i> with (d) <i>T. virens</i> (e) <i>T. harzianum</i>	170
Fig.4.5.6	(A) Analysis of RMSD for ligand and tomatinase complex (B) Analysis of RMSD ligands for tomatinase (C) Analysis of RMSD for ligand and PG2 complex (B) Analysis of RMSD ligands for PG2.	171
Fig.4.5.7	(A) RMSF Analysis of Ca during MD simulations for tomatinase enzyme; (B) RMSF Analysis of Ca during MD simulations for PG2 enzyme	173
Fig.4.5.8	(A) Radius of gyration between the ligand and PG2 complex; (B) Radius of gyration between the ligand and PG2 complex	174
Fig.4.5.9	(A) Solvent surface accessible area analysis of docked complexes; where control is the tomatinase enzyme; (B) Solvent surface accessible area analysis of docked complexes, where control is the PG2 enzyme	175

Fig.4.5.10	(A) Intermolecular hydrogen bonds distribution between the ligand and tomatinase complex; (B) Hydrogen bond number distribution between the ligand and tomatinase complex; (C) Intermolecular hydrogen bonds distribution between the ligand and PG2 complex; (D) Hydrogen bond number between the ligand and enzyme complex.	176
Fig. 5.1	Schematic representation of Nanosilica extraction from Paddy straw	181
Fig. 5.2	Synthesis of Nanosilica using straw ash combusted at 600°C for amorphous particles and at 900°C for crystalline particles.	182
Fig. 5.3	Schematic representation of synthesis of SiNPs employing aqueous extract of <i>S. mukorossi</i> via sol-gel method.	183
Fig. 5.4	Schematic representation of synthesis of SiNPs employing aqueous extract of <i>S. mukorossi</i> via sol-gel method and its application for development of Nanoencapsulation based formulation.	187
Fig. 5.5	XRD pattern (A) PS ash obtained at 600°C (B) PS ash obtained at 900°C. FTIR analysis (C) PS ash obtained at 600°C (D) PS ash obtained at 900°C	189
Fig. 5.6	EDX pattern (A) PS ash obtained at 600°C (B) PS ash obtained at 900°C	190
Fig. 5.7	Thermogravimetric Analysis of Paddy straw ash	190
Fig. 5.8	(A) Phytochemical screening of <i>S. mukorossi</i> seed pericarp aqueous extract (B) FTIR spectra of <i>S. mukorossi</i> seed pericarp	191 192
Fig. 5.9	UV Vis spectra of synthesized SiNPs (A) SiNPs synthesized using PSA obtained at 600°C (B) SiNPs synthesized using PSA obtained at 900°C (C) SiNPs synthesised employing aqueous extract of <i>S. mukorossi</i> .	193
Fig. 5.10	XRD Spectra (A) SiNPs synthesized using PSA-600 (B) SiNPs synthesized using PSA-900 (C) SiNPs synthesised employing aqueous extract of <i>S. mukorossi</i> from PS ash at 600°C.	194
Fig. 5.11	FTIR spectra (A) SiNPs synthesized using PSA-600 (B) SiNPs synthesized using PSA-900 (C) SiNPs synthesised employing aqueous extract of <i>S. mukorossi</i> from PS ash at 600°C.	195
Fig. 5.12	EDX analysis (A) SiNPs synthesized using PSA-600 (B) SiNPs synthesized using PSA-900 (C) SiNPs synthesised employing aqueous extract of <i>S. mukorossi</i> from PSA-600 (D) EDX mapping of the SiNPs synthesized using PSA-600 (E) EDX mapping of the SiNPs synthesized using PSA-900 (F) EDX mapping of the SiNPs synthesized employing aqueous extract of <i>S. mukorossi</i> .	196
Fig. 5.13	(A) FESEM micrographs of raw RS (B) Microscopic images of PSA-600 (C) Microscopic images of PSA-900 (D) TEM micrographs of PSA-600 (E) TEM micrographs of PSA-900 (F) FE-SEM micrographs of amorphous SiNPs (G) FE-SEM micrographs of crystalline SiNPs (H) TEM micrographs of amorphous SiNPs (I) TEM micrographs of crystalline SiNPs.	198
Fig. 5.14	Morphological characterization of SiNPs synthesised employing aqueous extract of <i>S. mukorossi</i> from PS-600 (A) FESEM micrographs (B) TEM micrographs (C) AFM analysis (D) Surface roughness	199

Fig. 5.15	Nitrogen adsorption-desorption isotherms (A) SiNPs synthesized using PSA-600 (B) SiNPs synthesized using PSA-900 (C) SiNPs synthesised employing aqueous extract of <i>S. mukorossi</i> from PSA-600	200
Fig. 5.16	(A) Zeta Potential Analysis of SiNPs (B) TG-DTA analysis of SiNPs (tested until 800°C) (C) Water Contact Angle of SiNPs	202
Fig. 5.17	Nitrogen adsorption-desorption isotherms of mesoporous SiNPs loaded with Clove oil (CO-SiNPs)	203
Fig. 5.18	Fourier transform infrared spectroscopy spectra of CO-SiNPs.	204
Fig. 5.19	<i>Fusarium oxysporum</i> mycelia inhibition using Clove oil and mesoporous SiNPs loaded with Clove oil (CO-SiNPs).	205
Fig. 5.20	Decolorization of methylene blue under the effect of UVC irradiation at different concentrations of SiNPs.	207
Fig. 5.21	First-order kinetics plot of dye degradation, denoted by (...) with SiNPs and by (----) without SiNPs.	208
Fig. 5.22	FTIR spectra of methylene blue after the photocatalytic degradation using Nanosilica	209
Fig. 6.1	A flow diagram depicting utilization of Paddy straw for in-house production and optimization of enzyme under SSF and its LCA	213
Fig. 6.2	<i>Trichoderma</i> strains used for lignocellulytic enzyme production	214
Fig. 6.3	Chitin estimation protocol	217
Fig. 6.4	Flow Diagram and System Boundary for the Solid-State Fermentation process	224
Fig. 6.5	Cellulase activity of <i>Trichoderma</i> strains	228
Fig. 6.6	Xylanase activity of <i>Trichoderma</i> strains	228
Fig. 6.7	Laccase activity of <i>Trichoderma</i> strains	229
Fig. 6.8	Plate culture of (A) <i>T. brevicompactum</i> (B) <i>T. asperellum</i> (C) Dual culture assay of <i>T. brevicompactum</i> and <i>T. asperellum</i>	229
Fig. 6.9	Chitin Biomass of fungal strains cultivated on PS in combination with DEOCs	230
Fig. 6.10	RSM optimization for xylanase production. Three dimensional plots showing (A) Effect of neem cake and time on xylanase activity using 8% paddy straw (B) Effect of paddy straw and neem cake on xylanase activity on 5 th day	233
Fig. 6.11	RSM optimization of cellulase production. Three dimensional plots showing (A) Effect of neem cake and time on cellulase activity using 8% PS (B) Effect of paddy straw and neem cake on cellulase activity	234
Fig. 6.12	RSM optimization for laccase production. Three dimensional plots showing (A) Effect of neem cake and time on laccase activity using 8% paddy straw (B) Effect of paddy straw and neem cake on laccase activity	236
Fig. 6.13	LCMS chromatogram of the most prominent band identified in the SDS-PAGE	239
Fig.6.14	Effect of (A) pH (B) Temperature (C) Thermal stability on xylanase production	242

Fig.6.15	Line-weaver Burk plot for determination of K_m and V_{max} of partially purified xylanase	244
Fig. 6.16	Reducing sugars released in different substrates treated with xylanase enzyme	245
Fig. 6.17	ReCiPe 2016 midpoint categories characterization results, for production of 1 kg xylanase	246
Fig. 6.18	ReCiPe 2016 midpoint categories normalization results for production of 1 kg xylanase	247
Fig. 6.19	FE-SEM micrographs at a magnification of 2500 and EHT 20 kV (A) Raw Paddy straw (PS) (B) Spent substrate	249
Fig. 6.20	FTIR spectra of the raw and treated substrate	251
Fig. 6.21	XRD spectra (A) Raw Paddy straw supplemented with Neem cake (8:3 ratio) (B) XRD spectra of the residual spent obtained after <i>Trichoderma</i> treatment	252
Fig. 6.22	Venn Diagram representation of different range of metabolites produced by (A) <i>T. brevicompactum</i> (B) <i>T. asperellum</i> (C) Microbial consortia	253
Fig. 6.23	Heat map representing % area of metabolites produced by <i>T.asperellum</i> (TA), <i>T. brevicompactum</i> (UP-91) and microbial consortia (MO)	258
Fig. 6.24	LCMS chromatogram of (A) <i>T. asperellum</i> (B) <i>T.brevicompactum</i> (C) Microbial consortia	259
Fig. 6.25	EDX profiling of the residual spent denoting the presence of Silica	266
Fig. 7.1	Interventions towards Paddy straw management and contribution towards SDGs	271

LIST OF TABLES

TABLE	PARTICULAR (S)	PAGE
Table 2.1	Application of <i>Trichoderma</i> against combating phytopathogen	44
Table 2.2	Commercially available formulations of <i>Trichoderma</i> spp.	51
Table 2.3	Extraction of nanosilica from Paddy agro-waste	54
Table 2.4	Application of Nanosilica in agriculture domain	59
Table 2.5	Use of Nanosilica for slow release of pesticides	65
Table 2.6	Degradation of pesticides using Nanosilica as a catalytic agent	70
Table 2.7	Photocatalytic degradation of textile dyes using Nanosilica	73
Table 2.8	Various pre-treatment approaches	77
Table 2.9	Different approaches adopted in biological pre-treatment	81
Table 2.10	Various enzymes produced by microorganisms on lignocellulosic biomass	86
Table 2.11	Production of lignocellulosic enzymes on agro-wastes under Solid and Submerged Fermentation	88
Table 3.1	Different substrate treatments used for <i>P. ostreatus</i> cultivation	100
Table 3.2	Physio-chemical properties of Paddy straw and different de-oiled cakes	104
Table 3.3	Nutritional parameters (%) for <i>P. ostreatus</i> fruit bodies harvested from PS supplemented with different de-oiled cakes	107
Table 3.4	Total Phenolic Content of <i>P. ostreatus</i> fruit bodies harvested from Paddy Straw supplemented with different de-oiled cakes	109
Table 3.5	Pearson's correlation coefficient between TPC and antioxidant activities	111
Table 3.6	Infrared bands observed in spent (PS+SC, PS) and Raw PS	114
Table 3.7	Spore count of <i>T. asperellum</i> cultivated on different substrate combinations	116
Table 3.8	Cost calculation of <i>P. ostreatus</i> cultivated on Paddy straw	117
Table 4.1	<i>In planta</i> assay to study the effect of different treatments for <i>Fusarium</i> wilt control in tomato plants	124
Table 4.2	Physio-chemical properties of Press Mud (PM) and Spent Mushroom Substrate	129
Table 4.3	GC-MS Profiling of secondary metabolites identified in Raw PS and SMS (PS+5%SC) treated with <i>T. asperellum</i>	132
Table 4.4	Multiple comparison analysis using Pearson correlation between various parameters observed under different treatments	148
Table 4.5	Survey result based on questionnaire of demonstration of bioformulation to farmers	152
Table 4.5.1	Statistics of evaluated 3D structure of tomatinase and PG2 protein	164
Table 4.5.2	Details of ligand molecules along with Auto Dock Score	168
Table 4.5.3	Average RMSD of backbone and ligand (Tomatinase enzyme)	172
Table 4.5.4	Average RMSD of backbone and ligand (PG2 enzyme)	172
Table 4.5.5	Free binding energy calculations for tomatinase enzyme and ligands complexes	177

Table 4.5.6	Free binding energy calculations for PG2 enzyme and ligands complexes	177
Table 5.1	FTIR bands observed in ashes and synthesised Nanosilica particles	194
Table 5.2	Cost analysis of synthesised Nanosilica using Paddy straw	210
Table 6.1	Design of experiments generated through central composite design and experimental responses under Response Surface Methodology	218
Table 6.2	Inventory of inputs and outputs for the LCA of Solid-State Fermentation Process	225
Table 6.3	ReCiPe 2016 Characterization (midpoint categories) results for 1 kg of enzyme production under Solid-State Fermentation	226
Table 6.4	Lignocellulolytic enzymes observed under CCD based model	231
Table 6.5	ANOVA analysis of xylanase production under CCD optimization	232
Table 6.6	ANOVA analysis of cellulase production obtained under CCD	234
Table 6.7	ANOVA analysis of laccase production under CCD	236
Table 6.8	Partial purification of xylanase enzyme	238
Table 6.9	FTIR spectra showing the band positions in control and treated samples	250
Table 6.10	GC-MS Profiling of secondary metabolites identified on PS treated with fungal cultures	255
Table 6.11	LCMS profiling of the residual spent	261

LIST OF ABBREVIATIONS

Symbol	Full Name
%	Percentage
°C	Degree Celsius
μ	Micro
μg	Microgram
μL	Microliter
3D	Three dimensional
a.i.	Active ingredients
AFM	Atomic Force Microscopy
BCA	Biocontrol agents
BET	Brunauer–Emmett–Teller
BSA	Bovine Serum Albumin
C	Carbon
C/N	Carbon and Nitrogen
CC	Castor cake
CCD	Central Composite Design
CFU	Colony Forming Units
CHN	Carbon, Hydrogen and Nitrogen
CMC	Carboxymethyl Cellulose
CNDs	Colloidal Nano delivery systems
CO	Clove oil
CRF	Central Research Facility
CTAB	Cetyltrimethyl ammonium bromide
DCB	Dichlorobenzene
DEOCs	De-oiled cakes
DLS	Dynamic Light Scattering
DMRT	Duncan’s multiple range test
DPPH	2,2-diphenyl-1-picrylhydrazyl
DSI	Disease Severity Index
dw	Dry weight
EDS	Energy Dispersive X-Ray Spectroscopy
EDTA	Ethylenediaminetetraacetic acid
EO	Essential Oil
EU	European Union
f.w.	Fresh weight
Fe	Iron
FE-SEM	Field Emission Scanning Electron Microscopy
Fig.	Figure

Symbol	Full Name
FOL	<i>Fusarium oxysporum lycopersici</i>
FPLC	Fast Protein Liquid Chromatography
FRAP	Ferric Reducing Antioxidant Power
FTIR	Fourier Transform Infrared spectrophotometry
g	Grams
GA	Gallic acid
GAE	Gallic acid equivalent
GC	Groundnut cake
GCMS	Gas chromatography–mass spectrometry
GHGs	Greenhouse gases
GOI	Government of India
GP	Germination Percentage
h	Hour
H ₂ SO ₄	Sulphuric acid
HCl	Hydrochloric acid
HPLC	High Performance Liquid Chromatography
IAA	Indole Acetic Acid
ICPMS	Inductively Couple Plasma Mass Spectrometry
IPM	Integrated Pest Management
ISR	Induced Systemic Response
JC	Jatropha cake
kDa	Kilodaltons
KOH	Potassium hydroxide
LCA	Life Cycle Assessment
LCMS	Liquid chromatography–mass spectrometry
m/z	Mass/Charge
m/z	Mass/charge
MB	Methylene Blue
MC	Mustard cake
mg	Milligrams
MIC	Minimum Inhibitory Concentration
min	Minutes
min	Minutes
mL	Milliliter
mm	Millimeter
mM	Millimolar
MSNs	Mesoporous silica nanoparticles
Mt	Million tons
NAG	N-acetyl glucosamine
NaOH	Sodium hydroxide

Symbol	Full Name
NC	Neem cake
nm	nanometers
NPK	Nitrogen Phosphorus Potassium
OECD	Organization for Economic Cooperation and Development
OHR-LCMS	Orbitrap High Resolution Liquid chromatography–mass spectrometry
<i>P. ostreatus</i>	<i>Pleurotus ostreatus</i>
PCA	Principal Component Analysis
PDA	Potato Dextrose Agar
PDI	Polydispersity Index
PE	Pickering Emulsions
PG2	Polygalacturonase
PGP	Plant Growth Promoting
PGPF	Plant Growth Promoting Fungi
PM	Particulate matters
PM	Press mud
ppm	Parts per million
PR	Pathogenesis Related
PS	Paddy straw
PSA	Paddy straw ash
psi	Pounds per square inch
ROS	Reactive oxygen species
rpm	Revolutions per minute
Rs.	Rupees
RSM	Response Surface Methodology
RT	Retention Time
SAIF	Sophisticated Analytical Instrument Facility
SAR	Systemic Acquired Resistance
SC	Soybean cake
SD	Standard deviation
SDGs	Sustainable Development Goals
SDS	Sodium Dodecyl Sulphate
sec	Seconds
Si	Silica
SiNPs	Nanosilica particles
SmF	Submerged State Fermentation
SMS	Spent Mushroom Substrate
SSF	Solid State Fermentation
TA	<i>Trichoderma asperellum</i>
TEM	Transmission Electron Microscopy

Symbol	Full Name
Temp.	Temperature
TGA	Thermogravimetric Analysis
TP	Talcum powder
TPC	Total Phenolic Content
TPTZ	2,4,6-tripyridyl-2-triazine
TSP	Total Soluble Protein
TSS	Total Soluble Sugars
U	Enzymatic Unit
U/g	Enzymatic units per gram substrate
UV-vis	Ultraviolet visible
v/v	Volume/volume
w/w	Weight/weight
XRD	X-ray diffraction
AQI	Air Quality Index
CRB	Crop Residue Burning
FAO	Food and Agriculture Organization
MNRE	Ministry of New and Renewable Energy
VIRRS	Visible Infrared Imaging Radiometer Suite
OECD	Organization for Economic Cooperation and Development
IPM	Integrated Pest Management
PDB	Protein Data Bank
CWDEs	Cell wall degrading enzymes
SPC	Simple Point Charge
RMSD	Root Mean Square Deviation
RMSF	Root Mean Square Fluctuation
SASA	Solvent Accessible Surface Area
STL	Standard Template Library
Rg	Radius of Gyration
SDF	Spatial Data File